# Streaming instabilities of intense charged particle beams propagating along a solenoidal magnetic field in a background plasma

Edward A. Startsev, Ronald C. Davidson, and Mikhail Dorf

*Plasma Physics Laboratory, Princeton University, Princeton, New Jersey 08543, USA*

Streaming instabilities of intense charged particle beams propagating along a solenoidal magnetic field in a background plasma are studied analytically and numerically. It is shown that the growth rate of the electromagnetic Weibel instability is modified by a relatively weak solenoidal magnetic field such that $\omega_{ce} > \beta_b \omega_{pe}$, where $\omega_{ce}$ is the electron gyrofrequency, $\omega_{pe}$ is the electron plasma frequency, and $\beta_b$ is the ion-beam velocity relative to the speed of light. Moreover, the Weibel instability is limited to very small propagation angles and long longitudinal wavelengths satisfying $k_\parallel^2 \ll k_\perp^2$ and $c^2 k_\parallel^2 \ll \omega_{pb}^2 \omega_{pi}^2/(\omega_{pb}^2 + \omega_{pi}^2)$, where $\omega_{pb}$ and $\omega_{pi}$ are the plasma frequencies of the beam ions and the background plasma ions, respectively. For shorter longitudinal wavelengths, the electrostatic lower-hybrid instability becomes dominant. In this paper, the growth rates of various electrostatic beam-plasma instabilities and the electromagnetic Weibel instability are compared, and the space-time development of the modified two-stream instability is studied in detail and compared with numerical simulations. © *2008 American Institute of Physics.* [DOI: 10.1063/1.2918673]

## I. INTRODUCTION

To achieve the high focal spot intensities necessary for high energy density physics and heavy ion fusion applications, the ion beam pulse[1–4] must be compressed transversely by a factor of 10 or more before it is focused onto the target. To achieve maximum compression, the space charge of the ion beam is neutralized by propagation of the beam pulse through a dense neutralizing background plasma.[5–10] If the space charge is fully neutralized by the plasma, the final compression is limited only by the initial temperature of the beam ions and possible collective processes[11–14] (such as the two-stream and filamentation instabilities) which may prevent full neutralization of the beam space charge. In one scenario,[5–10] transverse compression of the beam ions is facilitated by using solenoidal focusing magnets. Fields from the magnets can extend a large distance away from the solenoid into the neutralizing plasma and can change the nature of collective instabilities experienced by the compressing beam when it propagates through the neutralizing background plasma. Recent studies of the beam's charge and current neutralization in plasma with solenoidal magnetic field have shown that when the magnetic field is strong enough that $\omega_{ce} \sim \beta_b \omega_{pe}$, the electron dynamics becomes strongly affected by the magnetic field. Specifically, as shown in Ref. 15, if the condition $\omega_{ce} \sim \beta_b \omega_{pe}$ is satisfied, the magnetic field causes the plasma electrons to start rotating about the solenoid axis as they flow into the ion beam pulse to neutralize its charge and current. Because the magnetic field is frozen into the electron fluid, the electron rotation generates an azimuthal self-magnetic field $B_\theta$, which is much larger than in the case with no applied magnetic field. To balance the $v_\theta \times B_z$ Lorentz force on an electron fluid element due to its azimuthal rotation, the plasma is polarized to set up a radial electric field $E_r$. By applying an external magnetic field such that $\omega_{ce}/\beta_b \omega_{pe} \sim 1$, the total pinching force $F_r$

$= eZ_b(E_r - v_{zb}B_\theta)$ can be made much smaller than in the case with no applied field, which can be beneficial for beam transport. Also, the same rotation generates a solenoidal self-magnetic field which enhances the applied magnetic field, and makes the plasma have paramagnetic properties.

If $\omega_{ce} > \beta_b \omega_{pe}$, low-frequency helicon waves propagating almost transversely to the beam propagation direction can now be resonantly excited by the beam,[15] drastically changing the way current is being neutralized by the background plasma. Coupling to the helicon waves will also modify the electromagnetic filamentation (Weibel) instability.[16–19] In this paper we study in more detail the low-frequency electromagnetic and electrostatic streaming instabilities[20,21] of an intense ion beam propagating through background plasma along a solenoidal magnetic field. Because of the large ion mass, instabilities involving the ion cyclotron motion are very slow and will not be considered here. Therefore, in what follows we neglect the effect of the magnetic field on the beam and plasma ions, and only include its effects on the plasma electrons. In the analysis, we also treat all charged particle species in the cold-plasma approximation. One can neglect electron thermal effects if the directed ion beam velocity is much larger than the electron thermal speed $V_b \gg v_{th}^e$, and if the electron thermal speed is sufficiently small that $|\omega - k_\parallel V_e| \gg |k_\parallel|v_{th}^e$, and $|k_\perp|v_{th}^e \ll |\omega_{ce}|$. One can typically neglect ion thermal effects if the directed ion beam velocity is much larger than the thermal speed of the beam ions and the background ions, $V_s \gg v_{th}^s$, and if $|\omega - k_\parallel V_s| \gg |k|v_{th}^s$, where $s = (i, b)$ denotes the ions species. In the analysis that follows, these conditions are assumed to be satisfied.

The organization of this paper is the following. In Sec. II, the full electromagnetic linear dispersion relation is presented for an intense ion beam propagating through neutralizing background plasma along a solenoidal magnetic field. Conditions for the electromagnetic Weibel instability and the

electrostatic modified two-stream instabilities for nearly transverse propagation to the applied magnetic field are identified, and the growth rate of the Weibel instability modified by the solenoidal magnetic field is obtained. In Sec. III a detailed analysis of electrostatic modified two-stream instabilities is presented, and the unstable modes are identified and their frequency and growth rates are determined. Detailed numerical solutions to the dispersion relations are presented in Sec. IV. In Sec. V the space-time development of the modified two-stream instability is investigated, and the results are compared with numerical simulations using the particle-in-cell code LSP.[22,23] Finally, conclusions are summarized in Sec. VI.

## II. GENERAL DISPERSION RELATION AND THE ELECTROMAGNETIC FILAMENTATION (WEIBEL) INSTABILITY FOR $B_0 \neq 0$

For definiteness we assume that the beam velocity $V_b$ and externally applied magnetic field $\mathbf{B}_0 = B_0 \hat{\mathbf{e}}_z$ are directed along the $z$-direction. The wavenumber $\mathbf{k} = k_\perp \hat{\mathbf{e}}_x + k_\parallel \hat{\mathbf{e}}_z$ of the field perturbation is taken to be in the $(x, z)$ plane. We also assume that initially the background plasma electrons provide full charge and current neutralization, which requires the density of electrons to be $n_e = Z_i n_i + Z_b n_b$, and the electron drift velocity to be $V_e = Z_b V_b n_b / n_e$, where $n_s$ and $Z_s$ are the number density and charge state for the background ions ($s = i$) and beam ions ($s = b$). For simplicity, the subsequent analysis is carried out in a reference frame moving axially with the electrons. In this frame, $\bar{V}_b = V_b - V_e$, $\bar{V}_e = 0$, and $\bar{V}_i = -V_e$. Neglecting the cyclotron motion of the beam ions and plasma ions, the full cold-plasma dispersion relation for an ion beam propagating with velocity $V_b$ along the magnetic field $\mathbf{B}_0$ can be expressed as[20]

$$AN^4 + BN^2 + C = 0, \tag{1}$$

where $N = kc/\omega$ is the index of refraction, and $A$, $B$, and $C$ are defined by

$$A = \epsilon_{11} \sin^2 \theta + 2\epsilon_{13} \sin \theta \cos \theta + \epsilon_{33} \cos^2 \theta, \tag{2}$$

$$B = \epsilon_{13}^2 - \epsilon_{11}\epsilon_{33} - \epsilon_{11}\epsilon_{33}\cos^2 \theta - (\epsilon_{11}^2 + \epsilon_{12}^2)\sin^2 \theta - 2\epsilon_{13}\epsilon_{11}\sin \theta \cos \theta, \tag{3}$$

$$C = \epsilon_{33}(\epsilon_{11}^2 + \epsilon_{12}^2) - \epsilon_{11}\epsilon_{13}^2. \tag{4}$$

Here, $\theta$ is the angle between $\mathbf{k}$ and $\mathbf{B}_0 = B_0 \hat{\mathbf{e}}_z$, and $\epsilon_{ij}$ are the dielectric tensor elements defined by

$$\epsilon_{11} = 1 - \frac{\omega_{pe}^2}{\omega^2 - \omega_{ce}^2} - \frac{\omega_{pi}^2 + \omega_{pb}^2}{\omega^2}, \tag{5}$$

$$\epsilon_{12} = i \frac{\omega_{ce}\omega_{pe}^2}{\omega(\omega^2 - \omega_{ce}^2)}, \tag{6}$$

$$\epsilon_{13} = - \frac{\omega_{pi}^2}{\omega^2} \frac{k_\perp \bar{V}_i}{(\omega - k_\parallel \bar{V}_i)} - \frac{\omega_{pb}^2}{\omega^2} \frac{k_\perp \bar{V}_b}{(\omega - k_\parallel \bar{V}_b)}, \tag{7}$$

$$\epsilon_{33} = 1 - \frac{\omega_{pe}^2}{\omega^2} - \frac{\omega_{pi}^2}{\omega^2}\left[\frac{\omega^2 + (k_\perp \bar{V}_i)^2}{(\omega - k_\parallel \bar{V}_i)^2}\right] - \frac{\omega_{pb}^2}{\omega^2}\left[\frac{\omega^2 + (k_\perp \bar{V}_b)^2}{(\omega - k_\parallel \bar{V}_b)^2}\right], \tag{8}$$

where $k_\perp = k \sin \theta$, $k_\parallel = k \cos \theta$, $\omega_{ps}^2 = 4\pi q_s^2 n_s / m_s$ is the plasma frequency-squared for charge species $s = (e, i, b)$ with charge $q_s$ and mass $m_s$, and $\omega_{ce} = eB_0/m_e c$ is the electron cyclotron frequency.

For present purposes, we are interested in the regime corresponding to nearly transverse propagation with $\cos^2 \theta \ll 1$, and low-frequency perturbations with $|\omega| \ll \omega_{pe}, \omega_{ce}$. Even in this case the dispersion relation (1) is quite complicated. In what follows we analyze Eq. (1) in the short wavelength limit with $k^2 c^2 / \omega_{pe}^2 \gg 1$.

Making use of approximations enumerated in the previous paragraph, the dispersion relation (1) can be approximated by

$$1 + \frac{\omega_{pe}^2}{\omega_{ce}^2}\left[1 + \frac{\bar{\beta}_i^2 \omega_{pi}^2}{(\omega - k_\parallel \bar{V}_i)^2} + \frac{\bar{\beta}_b^2 \omega_{pb}^2}{(\omega - k_\parallel \bar{V}_b)^2}\right] - \frac{\omega_{pe}^2 \cos^2 \theta}{\omega^2}$$
$$- \frac{\omega_{pb}^2}{(\omega - k_\parallel \bar{V}_b)^2} - \frac{\omega_{pi}^2}{(\omega - k_\parallel \bar{V}_i)^2} = \frac{\omega_{pi}^2 \omega_{pb}^2 (\bar{\beta}_b - \bar{\beta}_i)^2}{(\omega - k_\parallel \bar{V}_b)^2 (\omega - k_\parallel \bar{V}_i)^2}, \tag{9}$$

where $\bar{\beta}_s = \bar{V}_s / c$ ($s = i, b$). The terms proportional to $\bar{\beta}_s^2$ in Eq. (9) describe transverse electromagnetic contributions that drive the so-called filamentation (Weibel) instability, whereas the rest of the terms in Eq. (9) represent electrostatic contributions. In the limit of sufficiently small solenoidal magnetic field that $\bar{\beta}_b^2 \omega_{pe}^2 / \omega_{ce}^2 \gg 1$, Eq. (9) reduces to

$$1 + \frac{\bar{\beta}_i^2 \omega_{pi}^2}{(\omega - k_\parallel \bar{V}_i)^2} + \frac{\bar{\beta}_b^2 \omega_{pb}^2}{(\omega - k_\parallel \bar{V}_b)^2} = 0. \tag{10}$$

Equation (10) corresponds to the dispersion relation for the Weibel instability in the absence of applied magnetic field. For $k_\parallel = 0$, note that Eq. (10) has a purely growing solution determined from[14]

$$\omega^2 = -\bar{\beta}_i^2 \omega_{pi}^2 - \bar{\beta}_b^2 \omega_{pb}^2. \tag{11}$$

In the opposite limit with strong magnetic field $\bar{\beta}_b^2 \omega_{pe}^2 / \omega_{ce}^2 \ll 1$, it is readily shown that Eq. (9) reduces to

$$1 + \frac{\omega_{pe}^2}{\omega_{ce}^2} - \frac{\omega_{pe}^2 \cos^2 \theta}{\omega^2} - \frac{\omega_{pb}^2}{(\omega - k_\parallel \bar{V}_b)^2} - \frac{\omega_{pi}^2}{(\omega - k_\parallel \bar{V}_i)^2}$$
$$= \frac{\omega_{pi}^2 \omega_{pb}^2 (\bar{\beta}_b - \bar{\beta}_i)^2}{(\omega - k_\parallel \bar{V}_b)^2 (\omega - k_\parallel \bar{V}_i)^2}. \tag{12}$$

For angles satisfying $\cos^2 \theta \gg \max(\omega_{pb}^2 / \omega_{pe}^2, \omega_{pi}^2 / \omega_{pe}^2)$, one can neglect the term on the right-hand side of Eq. (12), and the resulting dispersion relation becomes

$$1 + \frac{\omega_{pe}^2}{\omega_{ce}^2} - \frac{\omega_{pe}^2 \cos^2 \theta}{\omega^2} - \frac{\omega_{pb}^2}{(\omega - k_\parallel \bar{V}_b)^2} - \frac{\omega_{pi}^2}{(\omega - k_\parallel \bar{V}_i)^2} = 0. \tag{13}$$

Equation (13) describes the electrostatic modified two-stream instability between the plasma electrons and the beam ions or the plasma ions. In the opposite case of nearly transverse propagation such that $\cos^2 \theta < \max(\omega_{pb}^2/\omega_{pe}^2, \omega_{pi}^2/\omega_{pe}^2)$, and sufficiently large longitudinal wavenumbers that $c^2 k_\parallel^2 \gg \omega_{pb}^2 \omega_{pi}^2/(\omega_{pb}^2 + \omega_{pi}^2)$, Eq. (12) reduces to the equation describing an instability due to the interaction with lower-hybrid plasma oscillations, i.e.,

$$1 + \frac{\omega_{pe}^2}{\omega_{ce}^2} - \frac{\omega_{pb}^2}{(\omega - k_\parallel \bar{V}_b)^2} - \frac{\omega_{pi}^2}{(\omega - k_\parallel \bar{V}_i)^2} = 0. \tag{14}$$

Electrostatic instabilities described by Eqs. (13) and (14) will be considered in more detail in Sec. III.

In the opposite case when $c^2 k_\parallel^2 \ll \omega_{pb}^2 \omega_{pi}^2/(\omega_{pb}^2 + \omega_{pi}^2)$, Eq. (12) reduces to

$$- \frac{\omega_{pb}^2}{(\omega - k_\parallel \bar{V}_b)^2} - \frac{\omega_{pi}^2}{(\omega - k_\parallel \bar{V}_i)^2} = \frac{\omega_{pi}^2 \omega_{pb}^2 (\bar{\beta}_b - \bar{\beta}_i)^2}{(\omega - k_\parallel \bar{V}_b)^2 (\omega - k_\parallel \bar{V}_i)^2}, \tag{15}$$

which has an unstable solution

$$\omega = i(\bar{\beta}_b - \bar{\beta}_i) \frac{\omega_{pb} \omega_{pi}}{\sqrt{\omega_{pb}^2 + \omega_{pi}^2}} + ck_\parallel \left[ \frac{\bar{\beta}_b \omega_{pi}^2 + \bar{\beta}_i \omega_{pb}^2}{\omega_{pb}^2 + \omega_{pi}^2} \right] \tag{16}$$

describing a Weibel-type instability with finite $k_\parallel \neq 0$. The growth rate in Eq. (16) is modified compared to the case with weak magnetic field in Eq. (11) because the electrons are now magnetized, and the instability is between the beam ions and the background plasma ions. For arbitrary magnetic field strength, the normalized growth rate of the Weibel instability $\Gamma_B = \mathrm{Im}\,\omega/\sqrt{\omega_{pb}^2 + \omega_{pi}^2}$ calculated from Eq. (9) for $k_\parallel = 0$ is given by

$$\Gamma_B^2 = \frac{1}{2(1 + \omega_{pe}^2/\omega_{ce}^2)} \left\{ \frac{\omega_{pe}^2}{\omega_{ce}^2} \Gamma_0^2 - 1 + \left[ 4\left(1 + \frac{\omega_{pe}^2}{\omega_{ce}^2}\right) \Gamma_\infty^2 \right. \right.$$
$$\left. \left. + \left( \frac{\omega_{pe}^2}{\omega_{ce}^2} \Gamma_0^2 - 1 \right)^2 \right]^{1/2} \right\}, \tag{17}$$

where $\Gamma_B = \Gamma_0$ for $\bar{\beta}_b^2 \omega_{pe}^2/\omega_{ce}^2 \gg 1$, and $\Gamma_0 \equiv \mathrm{Im}\,\omega/\sqrt{\omega_{pb}^2 + \omega_{pi}^2}$ with $\mathrm{Im}\,\omega$ given by Eq. (11). Also, $\Gamma_B = \Gamma_\infty$ for $\bar{\beta}_b^2 \omega_{pe}^2/\omega_{ce}^2 \ll 1$, and $\Gamma_\infty \equiv \mathrm{Im}\,\omega/\sqrt{\omega_{pb}^2 + \omega_{pi}^2}$ with $\mathrm{Im}\,\omega$ given by Eq. (16) with $k_\parallel = 0$.

Here we examine stability properties only for the case of cold beam and plasma species. Thermal effects become important and can reduce the instability growth rate when the conditions summarized in Sec. I are not satisfied. For the Weibel instability these conditions imply that the electron thermal speed is small enough that $v_{\mathrm{th}}^e \ll V_b$ and $|k_\perp| v_{\mathrm{th}}^e \ll |\omega_{ce}|$, and the thermal speeds of the ion species are small enough that $|k_\perp| v_{\mathrm{th}}^s \ll \sqrt{\omega_{pb}^2 + \omega_{pi}^2} \Gamma_B$, where $s = (i, b)$ and $\Gamma_B$ is given by Eq. (17).

## III. ELECTROSTATIC MODIFIED TWO-STREAM INSTABILITY

As was shown in the previous section, the filamentation instability is limited to longitudinal wavenumbers $c^2 k_\parallel^2 \ll \omega_{pb}^2 \omega_{pi}^2/(\omega_{pb}^2 + \omega_{pi}^2)$. For large wavenumbers $c^2 k_\parallel^2 \gg \omega_{pb}^2 \omega_{pi}^2/(\omega_{pb}^2 + \omega_{pi}^2)$ and $c^2 k_\perp^2/\omega_{pe}^2 \gg 1$, the instability is nearly electrostatic and is described by the approximate dispersion relation[20]

$$1 - \frac{\omega_{pe}^2 \sin^2 \theta}{\omega^2 - \omega_{ce}^2} - \frac{\omega_{pe}^2 \cos^2 \theta}{\omega^2} - \frac{\omega_{pb}^2}{(\omega - k_\parallel \bar{V}_b)^2} - \frac{\omega_{pi}^2}{(\omega - k_\parallel \bar{V}_i)^2} = 0. \tag{18}$$

In Eq. (18), we have removed the small frequency assumption. When the beam density is zero ($\omega_{pb} = 0$) and $\cos^2 \theta > \omega_{pi}^2/\omega_{pe}^2$, Eq. (18) describes two types of waves with frequencies $\omega = \omega_\pm(\cos \theta)$ given by

$$\omega_\pm^2 = \tfrac{1}{2}[\omega_{ce}^2 + \omega_{pe}^2 \pm \sqrt{(\omega_{pe}^2 + \omega_{ce}^2)^2 - 4 \cos^2 \theta \omega_{ce}^2 \omega_{pe}^2}]. \tag{19}$$

The "+" sign corresponds to high-frequency oscillations with the frequency $\min(\omega_{ce}, \omega_{pe}) < \omega_+(\cos \theta) < \max(\omega_{ce}, \omega_{pe})$, and the "−" sign corresponds to lower-frequency oscillations. For nearly transverse propagation ($\theta \approx \pi/2$), it follows that

$$\omega_+ = \sqrt{\omega_{pe}^2 + \omega_{ce}^2}, \tag{20}$$

which is called the upper-hybrid frequency. On the other hand for $\theta \approx \pi/2$, the lower frequency $\omega_-$ can be approximated by

$$\omega_- = \frac{\omega_{pe} \cos \theta}{\sqrt{1 + \omega_{pe}^2/\omega_{ce}^2}}. \tag{21}$$

For angles such that $\cos^2 \theta < \omega_{pi}^2/\omega_{pe}^2$ one also needs to take into account the background ion response in Eq. (21). For these angles, the low-frequency oscillation is near the lower-hybrid frequency $\omega_{\mathrm{LH}}$ defined by

$$\omega_{\mathrm{LH}} = \frac{\omega_{pi}}{\sqrt{1 + \omega_{pe}^2/\omega_{ce}^2}}. \tag{22}$$

If the beam density is nonzero $\omega_{pb} \neq 0$, Eq. (18) describes two-stream instabilities where either the beam ions or the background plasma ions, streaming relative to the background electrons, can cause the instability. For $\cos^2 \theta > \omega_{pi}^2/\omega_{pe}^2$, expressing $\omega = k_\parallel \bar{V}_s + \eta_s$ ($s = \{i, b\}$), we obtain from Eq. (18),[20]

$$(\eta_s)_\pm = \pm \omega_{ps} \left[ \frac{k_\parallel^2 \bar{V}_s^2 (k_\parallel^2 \bar{V}_s^2 - \omega_{ce}^2)}{(k_\parallel^2 \bar{V}_s^2 - \omega_+^2)(k_\parallel^2 \bar{V}_s^2 - \omega_-^2)} \right]^{1/2}, \tag{23}$$

where instability exists for $k_\parallel^2 \bar{V}_s^2 < \omega_-^2$ or for $\omega_{ce}^2 < k_\parallel^2 \bar{V}_s^2 < \omega_+^2$. When the instability is resonant with $k_\parallel^2 \bar{V}_s^2 \approx \omega_\pm^2$, we obtain[20]

$$(\eta_s)_\pm^{\mathrm{res}} = \xi \left[ \frac{\omega_{ps}^2 \omega_\pm (\omega_\pm^2 - \omega_{ce}^2)}{2(\omega_+^2 - \omega_-^2)} \right]^{1/3}, \tag{24}$$

where

$$\xi = (-1 + i\sqrt{3})/2. \tag{25}$$

For present purposes, we refer to the instability with $\omega \approx \omega_+$ as the *upper-hybrid instability*, and the instability with $\omega \approx \omega_-$ as the *modified two-stream instability*.

For $\theta \approx \pi/2$ the low-frequency oscillation is at frequency $\omega \lesssim \omega_- \ll \omega_{ce}$ where $\omega_-$ is given by Eq. (21). In this case Eqs. (23) and (24) are simplified to become

$$(\eta_s)_- = \pm \omega_{ps}\left[\frac{k_\parallel^2 \bar{V}_s^2 \omega_{ce}^2}{(\omega_{pe}^2 + \omega_{ce}^2)(k_\parallel^2 \bar{V}_s^2 - \omega_-^2)}\right]^{1/2},$$

$$(\eta_s)_-^{\mathrm{res}} = \xi\left[\frac{\omega_{ps}^2 \omega_{ce}^2 \omega_-}{2(\omega_{pe}^2 + \omega_{ce}^2)}\right]^{1/3}$$

$$= \xi\omega_{\mathrm{LH}}\left(\frac{\omega_{ps}^2}{2\omega_{pi}^2}\right)^{1/3}\left[\cos\theta\left(\frac{\omega_{pe}}{\omega_{pi}}\right)\right]^{1/3}, \tag{26}$$

where $\omega_-$ is given by Eq. (21), and the resonance condition is $ck/\omega_{pe} \approx 1/\alpha_s$, where $\alpha_s \equiv \bar{\beta}_s\sqrt{1 + \omega_{pe}^2/\omega_{ce}^2}$.

When $\omega_{pe}^2 \gg \omega_{ce}^2$, the lower frequency branch becomes a short-wavelength ($k^2 c^2/\omega_{pe}^2 \gg 1$) helicon wave with $\omega \lesssim \omega_- \approx \omega_{ce}\cos\theta$ for all angles with $\cos^2\theta > \omega_{pi}^2/\omega_{pe}^2$. In this case, expressing $\omega = k_\parallel \bar{V}_s + (\eta_s)_-$, we obtain

$$(\eta_s)_- = \pm i\omega_{ce}\left(\frac{\omega_{ps}}{\omega_{pe}}\right)kr_c^s\left[\frac{1 - \cos^2\theta(kr_c^s)^2}{1 - (kr_c^s)^2}\right]^{1/2},$$

$$(\eta_s)_-^{\mathrm{res}} = \xi\omega_{ce}\left(\frac{\omega_{ps}^2}{2\omega_{pe}^2}\right)^{1/3}(\sin^2\theta\cos\theta)^{1/3}, \tag{27}$$

where $r_c^s \equiv \bar{V}_s/\omega_{ce}$, and the resonance condition is $k^2(r_c^s)^2 \approx 1$. The growth rate is a maximum at angle $\theta = \cos^{-1}(1/\sqrt{3}) = 54.7°$, and

$$\mathrm{Im}(\eta_s)_-^{\mathrm{max}} = \frac{1}{2}\omega_{ce}\left(\frac{\omega_{ps}^2}{\omega_{pe}^2}\right)^{1/3}. \tag{28}$$

For the high frequency branch, $\omega_{ce} < \omega \lesssim \omega_+ \approx \omega_{pe}$. Expressing $\omega = k_\parallel \bar{V}_s + (\eta_s)_+$ we obtain

$$(\eta_s)_+ = \pm i\omega_{pe}\left(\frac{\omega_{ps}}{\omega_{pe}}\right)\frac{k_\parallel r_p^s}{[1 - (k_\parallel r_p^s)^2]^{1/2}},$$

$$(\eta_s)_+^{\mathrm{res}} = \xi\omega_{pe}\left(\frac{\omega_{ps}^2}{2\omega_{pe}^2}\right)^{1/3}, \tag{29}$$

where the resonance condition is $k_\parallel^2(r_p^s)^2 \approx 1$. Note that this instability is independent of transverse wavenumber $k_\perp$, and has the same frequency and growth rate as in the absence of applied magnetic field ($\omega_{ce} = 0$).

In the opposite limit with $\omega_{pe}^2 \ll \omega_{ce}^2$, the lower frequency branch becomes $\omega_- = \omega_{pe}\cos\theta$ for all angles satisfying $\cos^2\theta > \omega_{pi}^2/\omega_{pe}^2$. In this case, expressing $\omega = k_\parallel \bar{V}_s + (\eta_s)_-$ with $k_\parallel \bar{V}_s \lesssim \omega_-$, we obtain

$$(\eta_s)_- = \pm i\omega_{pe}\left(\frac{\omega_{ps}}{\omega_{pe}}\right)\frac{kr_p^s}{[1 - (kr_p^s)^2]^{1/2}},$$

$$(\eta_s)_-^{\mathrm{res}} = \xi\omega_{pe}\left(\frac{\omega_{ps}^2\cos\theta}{2\omega_{pe}^2}\right)^{1/3}, \tag{30}$$

where $r_p^s \equiv \bar{V}_s/\omega_{pe}$ and the resonance condition is $k^2(r_p^s)^2 \approx 1$. The growth rate is a maximum at angle $\theta = 0$, and is given by

$$\mathrm{Im}(\eta_s)_-^{\mathrm{max}} = \frac{\sqrt{3}}{2}\omega_{pe}\left(\frac{\omega_{ps}^2}{2\omega_{pe}^2}\right)^{1/3}. \tag{31}$$

Note that in the case where $\omega_{pe}^2 \ll \omega_{ce}^2$, it is the instability for the lower frequency branch $\omega_-$ which has the same frequency and growth rate as the two-stream instability in the absence of an applied magnetic field, but only for $\theta = 0$.

For the high frequency branch with $\omega \approx \omega_+ \approx \omega_{ce}$, we find that $\omega_+^2 - \omega_{ce}^2 \approx \omega_{pe}^2\sin^2\theta$ and

$$(\eta_s)_+ = \pm i\omega_{pe}\left(\frac{\omega_{ps}}{\omega_{pe}}\right)\left[\frac{(k_\parallel r_c^s)^2 - 1}{1 + \left(\frac{\omega_{pe}}{\omega_{ce}}\right)^2\sin^2\theta - (k_\parallel r_c^s)^2}\right]^{1/2},$$

$$(\eta_s)_+^{\mathrm{res}} = \xi\omega_{pe}\left(\frac{\omega_{ps}^2\sin^2\theta}{2\omega_{pe}\omega_{ce}}\right)^{1/3}, \tag{32}$$

where the resonance condition is $(k_\parallel r_c^s)^2 \approx 1 + (\omega_{pe}/\omega_{ce})^2\sin^2\theta$. As one can see from Eq. (32), the instability has a very narrow bandwidth with $1 < (k_\parallel r_c^s)^2 < 1 + (\omega_{pe}/\omega_{ce})^2\sin^2\theta$. Thermal effects can be neglected provided $\bar{V}_s \gg v_{\mathrm{th}}^e$, $|k_\perp|v_{\mathrm{th}}^e \ll |\omega_{ce}|$. For the modified two-stream instability, the additional requirement is $\omega_{ps}/\omega_{pe} \gg v_{\mathrm{th}}^s/\bar{V}_s$. For the case of the upper-hybrid instability, the additional requirement is $\cos^2\theta \gg (\omega_+/\omega_{ps})^2(v_{\mathrm{th}}^s/\bar{V}_s)^2$.

So far we have examined electrostatic instabilities for sufficiently large propagation angles that $\cos^2\theta \gg \omega_{pi}^2/\omega_{pe}^2$ where we can neglect the contribution from the background plasma ions. In the opposite case, for sufficiently small angles of propagation that $\cos^2\theta \lesssim \omega_{pi}^2/\omega_{pe}^2$ and $\omega_{pi} \approx \omega_{pb}$, we estimate that

$$\mathrm{Re}\,\omega \sim \mathrm{Im}\,\omega \sim k_\parallel \bar{V}_b \sim \omega_{\mathrm{LH}}, \tag{33}$$

where the lower-hybrid frequency $\omega_{\mathrm{LH}}$ is defined in Eq. (22). For $\omega_{pb} \ll \omega_{pi}$, we express the solution to the dispersion relation as $\omega = k_\parallel \bar{V}_b + (\eta_b)_{\mathrm{LH}}$, where $(\eta_b)_{\mathrm{LH}}$ is defined by

$$(\eta_b)_{\mathrm{LH}} = \pm i\omega_{\mathrm{LH}}\frac{\omega_{pb}}{\omega_{pi}}\frac{k_\parallel r_{\mathrm{LH}}^b}{\left[1 + \frac{\omega_{pe}^2}{\omega_{pi}^2}\cos^2\theta - (k_\parallel r_{\mathrm{LH}}^b)^2\right]^{1/2}},$$

$$(\eta_b)_{\mathrm{LH}}^{\mathrm{res}} = \xi\omega_{\mathrm{LH}}\left(\frac{\omega_{pb}^2}{2\omega_{pi}^2}\right)^{1/3}\left(1 + \frac{\omega_{pe}^2}{\omega_{pi}^2}\cos^2\theta\right)^{1/6} \ll \omega_{\mathrm{LH}}. \tag{34}$$

Here, $(r_{\mathrm{LH}}^b)^2 \equiv \bar{V}_b^2/\omega_{\mathrm{LH}}^2$ and the resonance condition is $(k_\parallel r_{\mathrm{LH}}^b)^2 \approx 1 + (\omega_{pe}^2/\omega_{pi}^2)\cos^2\theta$. Thermal effects can be ne-
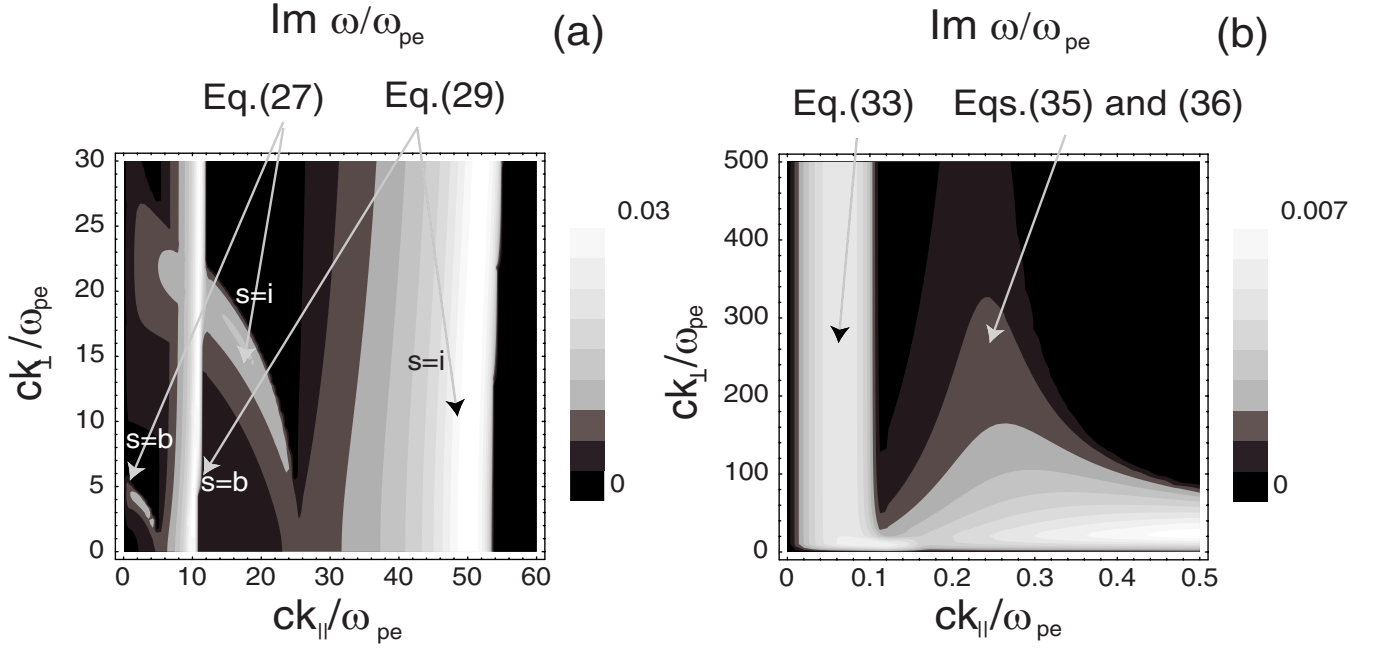
FIG. 1. (Color online) Contour plots of the normalized growth rate Im $\omega/\omega_{pe}$ of the electrostatic modified two-stream instability obtained from Eq. (1) plotted as a function of the normalized wavenumbers $ck_{\parallel}/\omega_{pe}$ and $ck_{\perp}/\omega_{pe}$ for the choice of system parameters $\bar{\beta}_b = \bar{V}_b/c = 0.1$, $\omega_{pb}/\omega_{pe} = 0.01$, $\omega_{pi}/\omega_{pb} = 1$, $\omega_{pe}/\omega_{ce} = 2$, and $n_b/n_i = 0.2$. (b) is an expanded view of (a) for $k_{\parallel}^2/k_{\perp}^2 < \omega_{pi}^2/\omega_{pe}^2$.

glected for this mode if $\bar{V}_b \gg v_{th}^e$, $|k_{\perp}|v_{th}^e \ll |\omega_{ce}|$ and $\cos^2 \theta \gg (v_{th}^b/\bar{V}_b)^2(1+\omega_{pi}^2/\omega_{pb}^2)$.

For $\cos^2 \theta \lesssim \omega_{pi}^2/\omega_{pe}^2$, there is also an instability due to the relative motion of the plasma ions and electrons. For $\cos^2 \theta \simeq \omega_{pi}^2/\omega_{pe}^2$, we estimate that

$$\text{Re } \omega \sim \text{Im } \omega \sim k_{\parallel}\bar{V}_i \sim \omega_{LH}. \tag{35}$$

For $\cos^2 \theta \ll \omega_{pi}^2/\omega_{pe}^2$, we can express $\omega = (\eta_i)_{LH}$, where $(\eta_i)_{LH}$ is given by

$$(\eta_i)_{LH} = \pm i\omega_{LH}\left(\frac{\omega_{pe}\cos\theta}{\omega_{pi}}\right)\frac{k_{\parallel}r_{LH}^i}{[1-(k_{\parallel}r_{LH}^i)^2]^{1/2}}, \tag{36}$$

$$(\eta_i)_{LH}^{res} = \xi\omega_{LH}\left(\frac{\omega_{pe}^2\cos^2\theta}{2\omega_{pi}^2}\right)^{1/3} \ll \omega_{LH}.$$

Here, $r_{LH}^i = \bar{V}_i/\omega_{LH}$ and the resonance condition is $(k_{\parallel}r_{LH}^i)^2 \approx 1$. We refer to the instability with $\omega \sim \omega_{LH}$ as the *lower-hybrid instability*. Thermal effects can be neglected for this mode if $\bar{V}_i \gg v_{th}^e$, $|k_{\perp}|v_{th}^e \ll |\omega_{ce}|$, and $\cos^2 \theta \gg \max[(v_{th}^i/\bar{V}_i)^2, (v_{th}^e/\bar{V}_i)^2(\omega_{pi}/\omega_{pe})^2]$.

Using Eq. (16), and Eqs. (26)–(32), we compare the maximum growth rates $\gamma_s^{max}$ of the instabilities that we have considered. To summarize, the ratio of the maximum growth rate of the lower-hybrid instability to the growth rate of the Weibel instability is

$$\frac{\gamma_{LH}^{max}}{\gamma_W} \sim \frac{1}{\bar{\beta}_b}\left(\frac{1+\omega_{pi}^2/\omega_{pb}^2}{1+\omega_{pe}^2/\omega_{ce}^2}\right)^{1/2}. \tag{37}$$

Similarly, the ratio of the maximum growth rate of the modified two-stream instability to the maximum growth rate of the lower-hybrid instability is

$$\frac{(\gamma_s)_-^{max}}{\gamma_{LH}^{max}} \sim \left(\frac{\omega_{ps}^2}{\omega_{pi}^2}\right)^{1/3}\left(\frac{\omega_{pe}}{\omega_{pi}}\right)^{1/3}. \tag{38}$$

Finally, the ratio of the maximum growth rate of the modified two-stream instability to the maximum growth rate of the upper-hybrid instability is

$$\frac{(\gamma_s)_-^{max}}{(\gamma_s)_+^{max}} \sim \begin{cases} \left(\dfrac{\omega_{ce}}{\omega_{pe}}\right)^{1/3}, & \omega_{ce} \gg \omega_{pe}, \\ \left(\dfrac{\omega_{ce}}{\omega_{pe}}\right), & \omega_{ce} \ll \omega_{pe}. \end{cases} \tag{39}$$

## IV. NUMERICAL SOLUTIONS TO DISPERSION RELATIONS

The growth rates of these instabilities have also been obtained by solving numerically the full electromagnetic dispersion relation in Eq. (1). Typical results are illustrated in Figs. 1–4 for $\bar{\beta}_b = \bar{V}_b/c = 0.1$, $\omega_{pb}/\omega_{pe} = 0.01$, $\omega_{pi}/\omega_{pb} = 1$, and $n_b/n_i = 0.2$. In Fig. 1, $\omega_{pe}/\omega_{ce} = 2$, and in Fig. 2, $\omega_{pe}/\omega_{ce} = 0.5$. Figures 1(a) and 2(a) show growth rate contour plots in the regions of large propagation angle with $\cos^2 \theta \gg \omega_{pi}^2/\omega_{pe}^2$. One can clearly see the instabilities due to the interaction of the beam ions and the background ions with lower frequency $\omega_-$ plasma oscillations {curved regions corresponding to $kr_c^s \approx 1$, $[s = (i,b)]$ in Fig. 1(a) and $kr_p^s \approx 1$ in Fig. 2(a)}, and with higher frequency $\omega_+$ plasma oscillations {vertically straight regions corresponding to $k_{\parallel}r_p^s \approx 1$, $[s = (i,b)]$ in Fig. 1(a), and $k_{\parallel}r_c^s \approx 1$ in Fig. 2(a)}. Figures 1(b) and 2(b) show growth rate contour plots in the regions of small propagation angle with $\cos^2 \theta \lesssim \omega_{pi}^2/\omega_{pe}^2$. One can
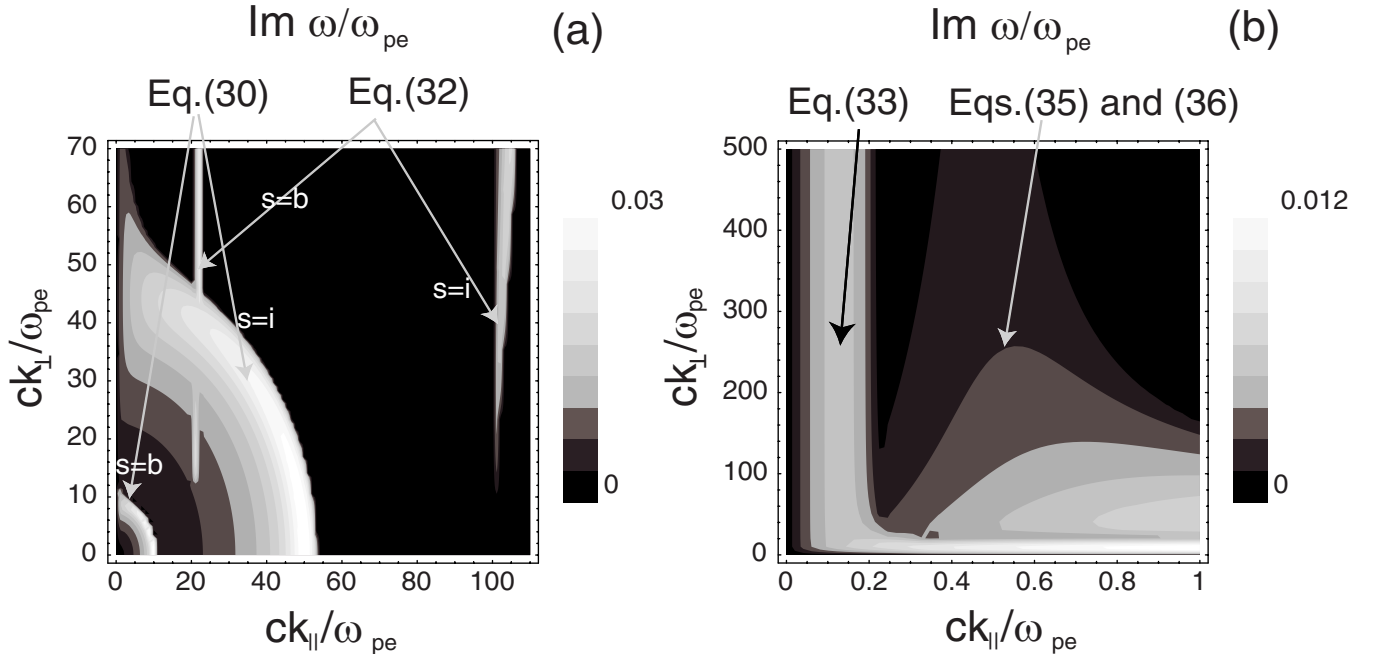
FIG. 2. (Color online) Contour plots of the normalized growth rate Im $\omega/\omega_{pe}$ of the electrostatic modified two-stream instability obtained from Eq. (1) plotted as a function of the normalized wavenumbers $ck_\parallel/\omega_{pe}$ and $ck_\perp/\omega_{pe}$ for the choice of system parameters $\bar{\beta}_b = \bar{V}_b/c = 0.1$, $\omega_{pb}/\omega_{pe} = 0.01$, $\omega_{pi}/\omega_{pb} = 1$, $\omega_{pe}/\omega_{ce} = 0.5$, and $n_b/n_i = 0.2$. (b) is an expanded view of (a) for $k_\parallel^2/k_\perp^2 < \omega_{pi}^2/\omega_{pe}^2$.

clearly see the instabilities due to the interaction of the beam ions ($k_\parallel r_{LH}^b \approx 1$) and background ions ($k_\parallel r_{LH}^i \approx 1$) with lower-hybrid plasma oscillations ($\omega \approx \omega_{LH}$). The regions of validity of the approximate analytical estimates obtained in Sec. III are illustrated by the arrows in Figs. 1 and 2.

Figure 3 shows the normalized growth rate Im $\omega/\omega_{pe}$ plotted as a function of the normalized wavenumber $ck_\parallel/\omega_{pe}$ for $ck_\perp/\omega_{pe} = 20$ and $\omega_{pe}/\omega_{ce} = 2$. The dotted line is the numerical solution of the full electromagnetic dispersion relation in Eq. (1), and the solid line is the solution of the (approximate) electrostatic dispersion relation in Eq. (18). As stated previously, for sufficiently strong magnetic field that
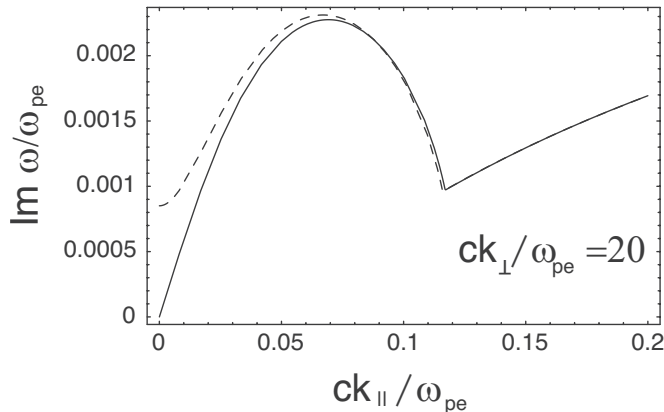
$\bar{\beta}_b \omega_{pe}/\omega_{ce} \ll 1$ and for transverse wavenumbers $c^2 k_\perp^2/\omega_{pe}^2 \gg 1$, the electrostatic dispersion relation is valid everywhere except for $c^2 k_\parallel^2 \ll \omega_{pb}^2 \omega_{pi}^2/(\omega_{pb}^2 + \omega_{pi}^2)$. In the region $c^2 k_\parallel^2 \ll \omega_{pb}^2 \omega_{pi}^2/(\omega_{pb}^2 + \omega_{pi}^2)$, the instability becomes an electromagnetic Weibel instability with growth rate given by Eq. (17). Figure 4 shows the normalized growth rate of the Weibel instability, Im $\omega/\sqrt{\omega_{pb}^2 + \omega_{pi}^2}$, plotted as a function of $\bar{\beta}_b \omega_{pe}/\omega_{ce}$. Figure 4 has been obtained by the solving the full electromagnetic dispersion relation in Eq. (1) (dotted line), and by using Eq. (17) (solid line) for the choice of system parameters $k_\parallel = 0$, $ck_\perp/\omega_{pe} = 20$, $\bar{\beta}_b = \bar{V}_b/c = 0.1$, $\omega_{pb}/\omega_{pe} = 0.01$, $\omega_{pi}/\omega_{pb} = 1$, and $n_b/n_i = 0.2$.
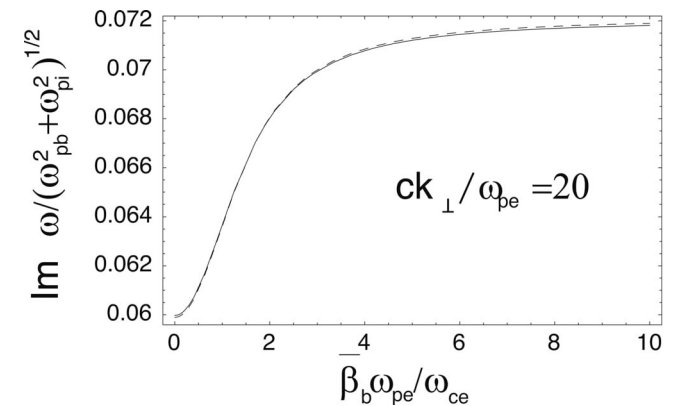


FIG. 3. Normalized growth rate Im $\omega/\omega_{pe}$ plotted as a function of normalized wavenumber $ck_\parallel/\omega_{pe}$ for $ck_\perp/\omega_{pe} = 20$, and $\bar{\beta}_b = \bar{V}_b/c = 0.1$, $\omega_{pb}/\omega_{pe} = 0.01$, $\omega_{pi}/\omega_{pb} = 1$, $\omega_{pe}/\omega_{ce} = 2$, and $n_b/n_i = 0.2$. The dotted line is the solution of the full electromagnetic dispersion relation in Eq. (1), and the solid line is the solution of the electrostatic dispersion relation in Eq. (18).



FIG. 4. Normalized growth rate of the Weibel instability Im $\omega/\sqrt{\omega_{pb}^2 + \omega_{pi}^2}$ plotted as a function of $\bar{\beta}_b \omega_{pe}/\omega_{ce}$ for $k_\parallel = 0$, $ck_\perp/\omega_{pe} = 20$, $\bar{\beta}_b = \bar{V}_b/c = 0.1$, $\omega_{pb}/\omega_{pe} = 0.01$, $\omega_{pi}/\omega_{pb} = 1$, and $n_b/n_i = 0.2$. The dotted line is the solution of the full electromagnetic dispersion relation in Eq. (1), and the solid line is obtained from Eq. (17).

## V. SPACE-TIME DEVELOPMENT OF ELECTROSTATIC MODIFIED TWO-STREAM INSTABILITY

In Secs. III and IV we provided a classification of possible electrostatic streaming instabilities. Because the frequency of the unstable perturbation is a function of wavenumber, an initial perturbation will grow and convect at the same time. The resulting shape of the phase-fronts can change with time and become quite complex. To illustrate the space-time development of the electrostatic modified two-stream instability, we consider here the instability due to the interaction of the beam ions with the lower frequency $\omega=\omega_-$ electrostatic oscillation given by Eq. (21) for small angles of propagation such that

$$\frac{\omega_{pi}^2}{\omega_{pe}^2} \ll \frac{k_\parallel^2}{k^2} \ll 1. \tag{40}$$

The asymptotic behavior of an initial perturbation can be studied using the Wentzel–Kramers–Brillouin (WKB) method[24] by extremizing the phase $\phi=\omega t-k_\parallel z-k_\perp x_\perp$ over all $k_\parallel$ and $k_\perp$, where $(\omega,k_\parallel,k_\perp)$ are related by the dispersion relation

$$1 + \frac{\omega_{pe}^2}{\omega_{ce}^2} = \frac{k_\parallel^2}{k_\perp^2+k_\parallel^2}\frac{\omega_{pe}^2}{\omega^2} + \frac{\omega_{pb}^2}{(\omega-k_\parallel V_b)^2}. \tag{41}$$

The asymptotic form of the initial perturbation amplitude $a$ can be expressed through the extremum phase as $a \sim \exp(\mathrm{Im}\ \phi)\exp(-i\ \mathrm{Re}\ \phi)$.

By expressing $k_\perp$ in terms of $k_\parallel$ and $y=\omega/k_\parallel V_b$, and using $\partial\phi/\partial k_\parallel=0$ and $\partial\phi/\partial y=0$, we obtain the extremum phase as a function of the normalized space-time coordinates $T=\omega^*t$, $\tau=\omega^*(t-z/V_b)$ and $x=x_\perp\omega^*/V_b$. We obtain

$$\phi = \epsilon\left[T - \frac{\tau}{(y-1)^2}\right]\sqrt{1+\left(\frac{x}{\tau}\right)^2\left(\frac{y-1}{y}\right)^4}, \tag{42}$$

where $y$ satisfies

$$\left(\frac{y-1}{y}\right)^5 [T(y-1)+\tau] = -\epsilon^2\tau\left(\frac{\tau}{x}\right)^2. \tag{43}$$

The angle of propagation is determined from

$$\cos\theta = \frac{k_\parallel}{k_\perp} = \left(\frac{y-1}{y}\right)\left(\frac{x}{\tau}\right). \tag{44}$$

Here, $\epsilon \equiv \omega_{pb}/\omega_{pe}$ and $\omega^* \equiv \omega_{pe}\omega_{ce}/\sqrt{\omega_{ce}^2+\omega_{pe}^2}$. For sufficiently large times that $T \sim x/\epsilon$ and $\tau \sim x$, the approximate solution for the angle $\theta$ is given by

$$\cos\theta \sim \epsilon^{1/2}\left[\frac{x^{2/3}}{(\epsilon T)^{1/6}\tau^{1/2}}\right], \tag{45}$$

which remains small so that $\omega_{pi}^2/\omega_{pe}^2 \sim \epsilon^2 \ll \cos^2\theta \ll 1$. This justifies using the dispersion relation for nearly transverse propagation $\theta \sim \pi/2$ in Eq. (41), and neglecting the contribution of the background ions. For the same $T \sim x/\epsilon$ and $\tau \sim x$, the approximate solution for the phase $\phi$ is given by

$$\mathrm{Re}\ \phi = \epsilon T - \frac{3}{4}x^{2/3}(\epsilon T)^{1/3} - \frac{3}{16}\frac{x^{4/3}}{(\epsilon T)^{1/3}}$$
$$- \epsilon^{1/2}\sqrt{3}x^{1/3}\tau^{1/2}(\epsilon T)^{1/6}, \tag{46}$$

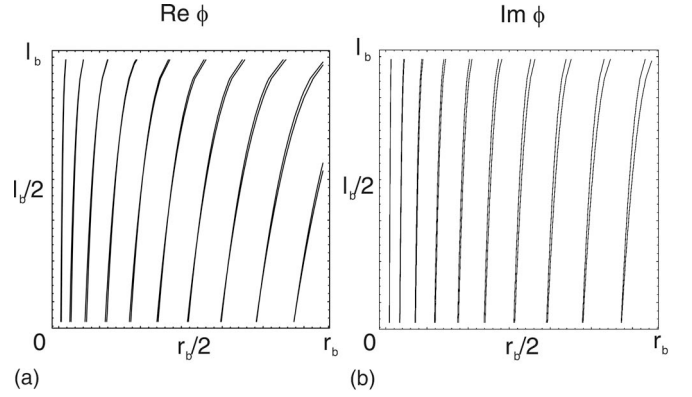FIG. 5. Contour plots of (a) Re $\phi$ and (b) Im $\phi$ of the extremal phase $\phi$ at time $t=(\omega_{pe}/\omega_{pb})l_b$ plotted for $\beta_b=0.2$, $n_b/n_{e0}=0.5$, $\omega_{ce}/\omega_{pe}=1.4$, bunch radius $r_b=1.5c/\omega_{pe}$, and bunch length $l_b=10r_b$.

$$\mathrm{Im}\ \phi = \frac{3\sqrt{3}}{4}x^{2/3}(\epsilon T)^{1/3} - \frac{3\sqrt{3}}{16}\frac{x^{4/3}}{(\epsilon T)^{1/3}}$$
$$+ \epsilon^{1/2}x^{1/3}\tau^{1/2}(\epsilon T)^{1/6}. \tag{47}$$

Figure 5 shows contour plots of Re $\phi$ [Fig. 5(a)] and Im $\phi$ [Fig. 5(b)] of the extremal phase $\phi$ at time $t=(\omega_{pe}/\omega_{pb})l_b$ plotted for $\beta_b=0.2$, $n_b/n_{e0}=0.5$, $\omega_{ce}/\omega_{pe}=1.4$, bunch radius $r_b=1.5c/\omega_{pe}$, and bunch length $l_b=10r_b$, where $n_{e0}$ is the ambient electron density. In Figs. 5(a) and 5(b), the approximate analytical solutions in Eqs. (46) and (47) are superposed on the numerical solution of Eqs. (42) and (43). The amplitude $a$ of the unstable perturbation is proportional to $a \sim \exp(\mathrm{Im}\ \phi)\exp(-i\ \mathrm{Re}\ \phi)$. Therefore, the perturbation phase-fronts correspond to curves of constant phase Re $\phi$ =const [see Fig. 5(a)]. The instability exists only inside the beam. Further shaping of the phase-fronts takes place outside of the pulse where the perturbation amplified by the instability inside of the pulse propagates away with group velocity $\mathbf{v}_g=\partial\omega/\partial\mathbf{k}$ satisfying

$$\frac{\partial\omega}{\partial\mathbf{k}}\cdot\mathbf{k} = 0. \tag{48}$$

Equation (48) is valid for both electrostatic oscillation branches $\omega=\omega_\pm(\cos\theta)$.

Figure 6 shows the results of simulations obtained using the particle-in-cell (PIC) simulation code LSP for a potassium $K^+$ ion beam propagating through neutralizing background plasma (upward direction) along a solenoidal magnetic field pointing in the $y$-direction for several values of magnetic field strength corresponding to $\omega_{ce}/\omega_{pe}=0,0.7,1.4$.[8] The simulations using the LSP code were carried out for the following parameters: ambient electron density $n_{e0}=10^{11}$ cm$^{-3}$; grid size along the direction of beam propagation $\omega_{pe}\Delta y/c=0.12$; grid size transverse to the direction of beam propagation $\omega_{pe}\Delta x/c=0.06$; time step $\omega_{pe}\Delta t=0.05$; and with nine particles per cell for every species.

Figure 6 shows contour plots of the normalized electron density $n_e/n_{e0}$ including collective excitations for $\beta_b=0.2$, $n_b/n_{e0}=0.5$, bunch radius $r_b=1.5c/\omega_{pe}$, and bunch length $l_b=10r_b$. Here, $n_{e0}$ is the ambient electron density. The charac-
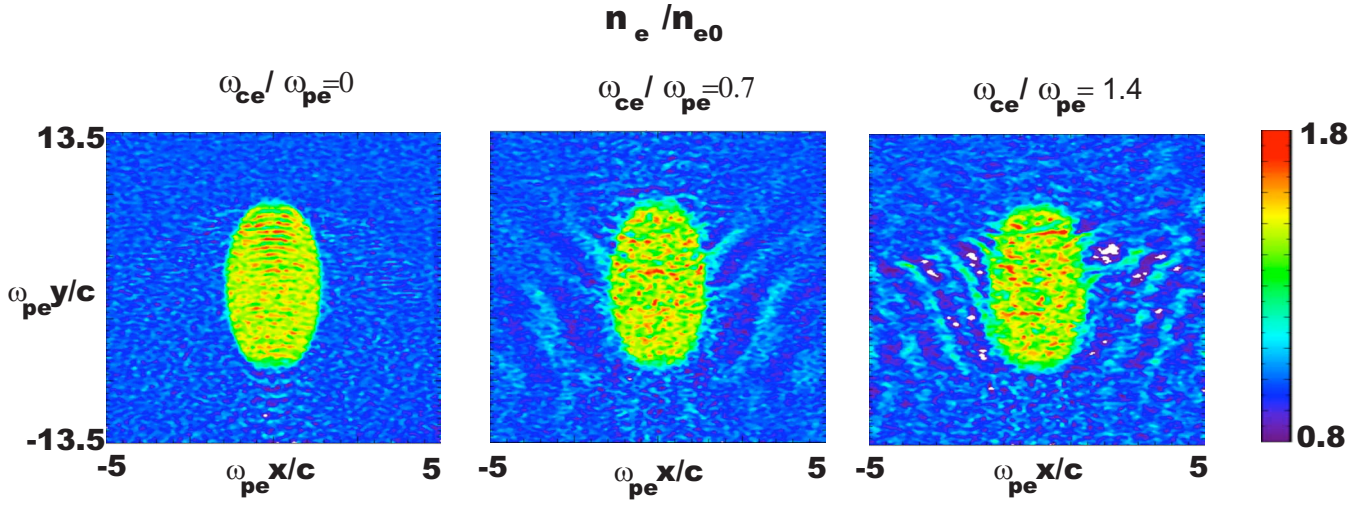
$$n_e / n_{e0}$$



FIG. 6. (Color online) Color plot of the normalized electron density $n_e/n_{e0}$ including collective excitations obtained using LSP simulations of a potassium K$^+$ ion beam propagating in neutralizing background plasma upward along a solenoidal magnetic field pointing in the $y$-direction for $\beta_b=0.2$, $n_b/n_{e0}=0.5$, $r_b=1.5c/\omega_{pe}$, and $l_b=10r_b$ and several values of magnetic field strength corresponding to $\omega_{ce}/\omega_{pe}=0,0.7,1.4$.

teristic shape of the phase-fronts (curves of maximum density) is similar to what is found using an asymptotic analysis of the instability [compare Figs. 5(a) and 6].

## VI. CONCLUSIONS

To summarize, in the present paper we have studied electromagnetic (Weibel) and electrostatic (two-stream) instabilities of an intense charged particle beam propagating along a solenoidal magnetic field in a background plasma in the limit $c^2k^2/\omega_{pe}^2 \gg 1$. It has been shown that the growth rate of the electromagnetic Weibel instability is modified by a small-amplitude solenoidal magnetic field such that $\omega_{ce}^2 > \beta_b^2 \omega_{pe}^2$, and the instability becomes limited to very small propagation angles with $c^2 k_\parallel^2 \lesssim \omega_{pb}^2 \omega_{pi}^2/(\omega_{pb}^2 + \omega_{pi}^2)$. For large longitudinal wavenumbers, the instability becomes the low-frequency electrostatic lower-hybrid instability with a growth rate that is $\omega_{ce}/\beta_b \omega_{pe}$ times larger than the growth rate of the Weibel instability. For larger angles with $\cos^2\theta > \omega_{pi}^2/\omega_{pe}^2$, the instability growth rate is proportional to $[\cos\theta(\omega_{pe}/\omega_{pi})]^{1/3}$.

We have also studied the asymptotic space-time development of the modified two-stream instability using a WKB analysis. The results of the analysis have shown that the phase-fronts of the unstable perturbation have a somewhat peculiar shape shown in Fig. 5, which is similar to what is found in numerical simulations using the LSP code (Fig. 6).

Even though electrostatic streaming instabilities typically have much larger growth rates than the Weibel instability, they require that a resonance condition be satisfied for maximum growth. If the ion beam is being compressed transversely by an external magnetic field while the instability is developing, the compression of the ion beam can cause changes in the unstable perturbation wavenumbers (transverse $k_\perp$ and longitudinal $k_\parallel$).[25,26] This in turn can result in a *detuning* of the resonant electrostatic two-stream instabilities, thereby making them much less dangerous. The study of these detuning effects on the modified two-stream instabilities is underway, and will be reported in future publications.

[1] R. C. Davidson and H. Qin, *Physics of Intense Charged Particle Beams in High Energy Accelerators* (World Scientific, Singapore, 2001), and references therein.

[2] M. Reiser, *Theory and Design of Charged Particle Beams* (Wiley, New York, 1994).

[3] A. W. Chao, *Physics of Collective Beam Instabilities in High Energy Accelerators* (Wiley, New York, 1993).

[4] R. C. Davidson, *Physics of Non-Neutral Plasmas* (World Scientific, Singapore, 2001), and references therein.

[5] P. K. Roy, S. S. Yu, E. Henestroza, A. Anders, F. M. Bieniosek, J. Coleman, S. Eylon, W. G. Greenway, M. Leither, B. G. Logan, W. L. Waldron, D. R. Welch, C. Thoma, A. B. Sefkow, E. P. Gilson, P. C. Efthimion, and R. C. Davidson, Phys. Rev. Lett. **95**, 234801 (2005).

[6] B. G. Logan, F. M. Bieniosek, C. M. Celata, J. Coleman, W. Greenway, E. Henestroza, J. W. Kwan, and P. K. Roy, Nucl. Instrum. Methods Phys. Res. A **577**, 1 (2007).

[7] I. D. Kaganovich, A. B. Sefkow, E. A. Startsev, R. C. Davidson, and D. R. Welch, Nucl. Instrum. Methods Phys. Res. A **577**, 93 (2007).

[8] I. D. Kaganovich, E. A. Startsev, A. B. Sefkow, and R. C. Davidson, "Controlling charge and current neutralization of an ion beam pulse in a background plasma by application of a solenoidal magnetic field. I. Limit of small magnetic field," Phys. Plasmas (submitted).

[9] A. B. Sefkow, R. C. Davidson, I. D. Kaganovich, E. P. Gilson, P. K. Roy, P. A. Seidl, S. S. Yu, and J. J. Barnard, Nucl. Instrum. Methods Phys. Res. A **577**, 289 (2007).

[10] D. R. Welch, D. V. Rose, C. Thoma, A. B. Sefkow, I. D. Kaganovich, P. A. Seidl, S. S. Yu, and P. K. Roy, Nucl. Instrum. Methods Phys. Res. A **577**, 231 (2007).

[11] E. A. Startsev and R. C. Davidson, Phys. Plasmas **13**, 062108 (2006).

[12] H. Qin, E. A. Startsev, and R. C. Davidson, Phys. Rev. ST Accel. Beams **6**, 014401 (2003).

[13] H. Qin, Phys. Plasmas **10**, 2708 (2003).

[14] R. C. Davidson, I. D. Kaganovich, H. Qin, and E. A. Startsev, Phys. Rev. ST Accel. Beams **7**, 114801 (2004).

[15] I. D. Kaganovich, E. A. Startsev, A. B. Sefkow, and R. C. Davidson, Phys. Rev. Lett. **99**, 235002 (2007).

[16] E. S. Weibel, Phys. Rev. Lett. **2**, 83 (1959).

[17] R. C. Davidson, D. A. Hammer, I. Haber, and C. E. Wagner, Phys. Fluids **15**, 317 (1972).

[18] R. Lee and M. Lampe, Phys. Rev. Lett. **31**, 1390 (1973).

[19] C. A. Kapetanakos, Appl. Phys. Lett. **25**, 484 (1974).

[20] A. I. Ahiezer, I. A. Ahiezer, R. V. Polovin, A. G. Sitenko, and K. N. Stepanov, *Plasma Electrodynamics* (Nauka, Moscow, 1974).

[21] T. H. Stix, *Waves in Plasmas* (AIP, New York, 1992).

[22] LSP is a software product of Voss Scientific, www.vosssci.com, Albuquerque, NM 87108.

[23] T. P. Hughes, S. S. Yu, and R. E. Clark, Phys. Rev. ST Accel. Beams **2**, 110401 (1999).

[24] R. Briggs, *Advances in Plasma Physics*, edited by A. Symon and W. B. Thompson (Interscience, New York, 1971), Vol. 4, p. 43.

[25] E. A. Startsev and R. C. Davidson, Phys. Plasmas **13**, 062108 (2006).

[26] E. P. Lee, S. Yu, H. L. Buchanan, F. W. Chambers, and M. N. Rosenbluth, Phys. Fluids **23**, 2095 (1980).